

Formation of Ferromagnetic FePt Nanoparticles by Ion Implantation

C. W. White, S. P. Withrow, J. D. Budai, L. A. Boatner, K. D. Sorge, J. R. Thompson, K. S. Beaty¹, and A. Meldrum¹

Oak Ridge National Laboratory, Oak Ridge, TN 37831

¹The University of Alberta, Edmonton, Alberta, Canada

ABSTRACT

Oriented ferromagnetic FePt nanoparticles with the face-centered tetragonal $L1_0$ structure were produced in Al_2O_3 single crystal hosts by ion implantation and annealing. Both the orientation and particle-size of the FePt particles depend strongly on the implantation conditions. The magnetic coercivities are extremely high, reaching values in excess of 20 kOe for Pt concentrations of ~45% in the FePt alloy. Ferromagnetic FePt nanoparticles were also produced in amorphous SiO_2 by ion implantation and annealing.

INTRODUCTION

Materials with a high magnetocrystalline anisotropy have recently generated considerable interest since these materials are excellent candidates for ultrahigh-density magnetic data storage applications [1]. Intermetallic, chemically ordered alloys of FePt and CoPt exist in the face centered tetragonal (fct) $L1_0$ structure. This structure consists of alternating planes of Fe (Co) atoms and Pt atoms stacked along the $\langle 001 \rangle$ direction of the crystal, and this arrangement gives rise to a very high magnetocrystalline anisotropy. Consequently, high magnetic coercivities should be achievable in nanoparticles of these materials even down to very small grain sizes. Nanoparticles of FePt have previously been synthesized chemically as a superlattice of monodispersed spherical particles [2] and FePt nanoparticles have been incorporated into amorphous Al_2O_3 [3, 4], SiO_2 [5], Be_2O_3 [6], and Si_3N_4 [7]. In this work, we have used ion implantation followed by thermal annealing to produce oriented Fe_xPt_{1-x} nanoparticles embedded in the near surface region of single-crystal Al_2O_3 [8]. The nanoparticles are ferromagnetic and can exhibit an extremely high magnetic coercivity (>20 kOe) depending on the Fe/Pt ratio. The formation of ferromagnetic Fe_xPt_{1-x} nanoparticles in amorphous SiO_2 is also demonstrated.

EXPERIMENTAL PROCEDURE

Single crystals of c -axis-oriented (0001) Al_2O_3 were used in this work. The sequential implantation of Fe (350 keV) and Pt (910 keV) ions was used to produce overlapping concentration profiles at a projected range of ~170 nm. The Fe dose was fixed at $1 \times 10^{17}/cm^2$ and the Pt dose was chosen to produce the desired Pt atomic fraction x [where $x = Pt/(Fe + Pt)$] in the alloy. Samples were implanted either at high temperature (550°C for Fe and 500°C for Pt) or at a lower temperature (200°C for Fe and Pt). Implantation at elevated temperatures was used to try to maintain crystallinity in the matrix during implantation. Implanted samples were annealed at 1100°C for 2 hours in flowing Ar + 4% H_2 followed by slow cooling. The samples were characterized by Rutherford backscattering (RBS)-ion channeling (2.3 MeV He^+), by x-ray diffraction (Cu K radiation using both four-circle and powder diffractometers), and by transmission electron microscopy (TEM). A SQUID magnetometer was used to determine

magnetic properties in the temperature range of 5–400 K in applied magnetic fields up to 65 kOe.

RESULTS

An x-ray spectrum and cross-section micrograph are shown in Fig. 1 for a Pt-rich alloy sample ($\text{Fe}_{48}\text{Pt}_{52}$) that was formed by implantation at 550°C followed by annealing. The ω -scans along the c -axis of Al_2O_3 (Fig. 1a) show the expected strong diffraction from Al_2O_3 , in addition to numerous other lines – all of which arise from FePt. These results show that, not only have FePt nanoparticles been formed by implantation, but that the nanoparticles are oriented with respect to the Al_2O_3 matrix. Several orientations of the FePt particles are evident in Fig. 1a when the implantation is carried out at this elevated temperature. In the x-ray lines arising from FePt, there are several superlattice reflections (denoted by s) along with several fundamental reflections. The existence of the superlattice reflections demonstrates that at least part of the nanoparticles have the ordered fct $L1_0$ structure, and it is likely that all of the FePt nanoparticles are in this chemically ordered phase. A qualitative measure of the degree of ordering is given by the order parameter which can be estimated by comparing the integrated intensity in the superlattice reflection to that in the corresponding fundamental reflection. In Fig. 1, the order parameter approaches unity for both (001) and (110) oriented nanoparticles. Figure 1b shows the microstructure in the near-surface region. The FePt nanoparticles are in the size range 2–10 nm in diameter with a few nanoparticles as large as 25 nm.

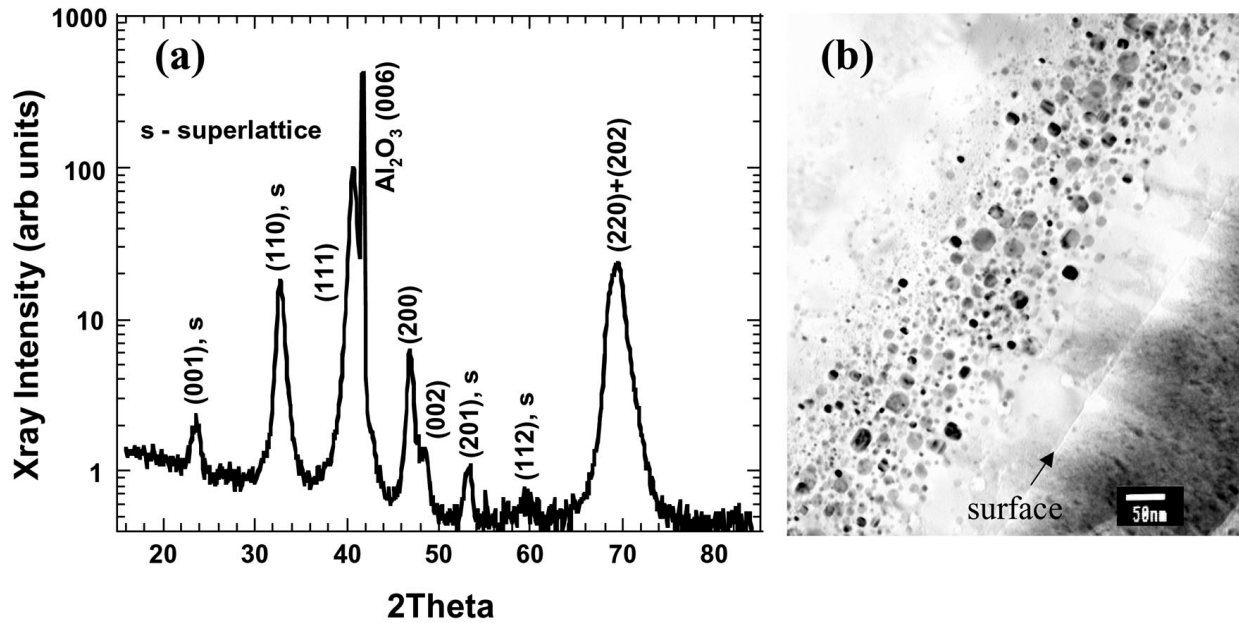


Figure 1. X-ray diffraction (a) and cross-section TEM (b) results for c -axis Al_2O_3 implanted by Fe (350 keV, $1 \times 10^{17}/\text{cm}^2$, 550°C) + Pt (910 keV, $1.1 \times 10^{17}/\text{cm}^2$, 500°C) followed by annealing ($1100^\circ\text{C}/2 \text{ h}/\text{Ar} + 4\% \text{ H}_2$).

Alloying of Fe and Pt leads to nanoparticles with an extremely high magnetic coercivity. Figure 2 shows magnetization measurements following annealing for samples implanted by Fe only, by Pt only, and with the combination of Fe + Pt (in the alloy composition of Fe₅₅Pt₄₅). For these results, a superconducting SQUID magnetometer was used to measure the magnetic moment of the sample (at 5 K) as the applied field was scanned in the range ± 65 kOe. (The diamagnetic background of Al₂O₃ has been removed from all of the magnetization measurements in this work.) From the results of Fig. 2, if Fe alone is implanted the magnetic coercivity is only 140 Oe. If Pt alone is implanted, the coercivity is essentially zero. However, in the case of the Fe₅₅Pt₄₅ alloy, the magnetic coercivity is in excess of 20 kOe. This very high coercivity results because the FePt alloy has the fct L1₀ structure.

Magnetization measurements for the Fe₅₅Pt₄₅ alloy in two different field orientations are shown in Fig. 3a. The coercive field is in excess of 20 kOe with H normal to the surface and almost 15 kOe with H parallel to the surface. These values are probably lower limits since the magnetization may not be saturated even at a field of 65 kOe. The fact that the magnetization measurements are similar for both orientations is reasonable since very few of the particles are oriented with the easy axis of magnetization ($\langle 001 \rangle$) normal to the surface. For both field orientations, there is a pronounced shoulder near H = 0. A similar feature has been observed by others [9, 10], but further research is required in order to clarify this behavior.

The Pt concentration in the alloy can be changed by varying the Pt implant dose, and Fig. 3b shows the measured variation of H_c with Pt concentration. H_c reaches a maximum at $\sim 45\%$ and then decreases rapidly on either side. At a Pt concentration of $\sim 25\%$, the coercive field is nearly zero, but in this case, the x-ray diffraction results are consistent with those expected from Fe₃Pt which is an ordered alloy with the cubic L1₂ structure. The other samples reported in Fig. 3b have an x-ray spectrum that is expected for the fct L1₀ structure of FePt. This dependence on Pt concentration is similar to that reported by others [2] but the coercive fields in Fig. 3b are considerably higher than those reported in refs. [2–7].

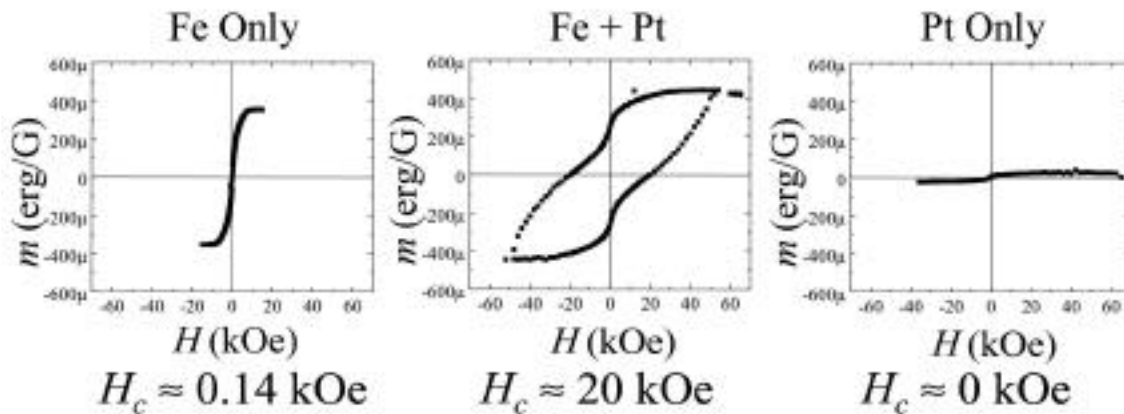


Figure 2. Magnetization measurements (at 5 K with H normal to the surface) for Al₂O₃ samples implanted with Fe only, with Pt only, and with Fe + Pt (in the alloy composition Fe₅₅Pt₄₅).

The FePt nanoparticle orientation and microstructure can be changed significantly by reducing the implantation temperature to 200°C (or below) as demonstrated in Fig. 4. In the x-ray diffraction results (4a), the only alloy line observed following annealing is a very intense

FePt (111) reflection showing that essentially all of the FePt nanoparticles are oriented with their $\langle 111 \rangle$ axis parallel to the c -axis of Al_2O_3 . Consequently, a single orientation of nanoparticles is produced by these implantation and annealing conditions. In addition, the particle size (Fig. 4b) is much larger in the sample implanted at 200°C than that observed after the high-temperature implantation (Fig. 1b). Particles up to 2000 nm in length parallel to the surface are observed in Fig. 4b, and particle thickness is ~ 25 nm. RBS-channeling measurements show that a buried amorphous layer is formed during implantation at 200°C , but not in the samples implanted at high temperature. Channeling measurements also demonstrate that this buried amorphous layer crystallizes during annealing. This suggests that crystallization occurs from both interfaces during annealing accompanied by the segregation of Fe and Pt into a thin layer of high concentration thus forming the large particles seen in Fig. 4b. The shape of these particles suggests that locally the percolation threshold has been exceeded. Magnetization measurements on the sample implanted at 200°C give a coercive field of $H_c \sim 24$ kOe at 5 K (for both field orientations). This is only slightly greater than that of the nanocomposite produced by implantation at the high temperature, even though microstructure and particle size are considerably different.

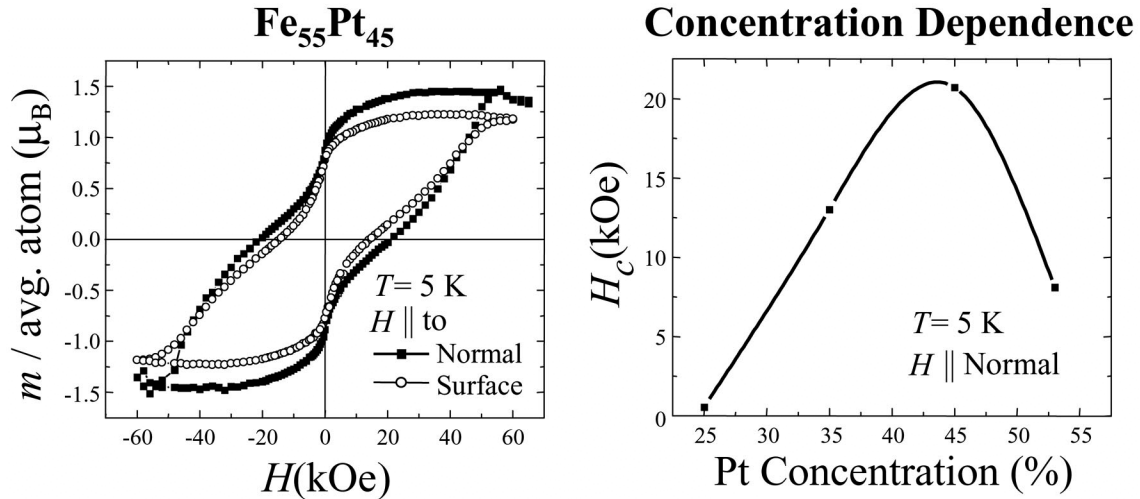


Figure 3. Magnetic properties of $\text{Fe}_{1-x}\text{Pt}_x$ nanoparticles in Al_2O_3 . Magnetization curves for $\text{Fe}_{55}\text{Pt}_{45}$ are shown in 3a for two orientations of the applied field. The variation of H_c with alloy composition is shown in 3b.

FePt nanoparticles can also be produced in other matrices by implantation and annealing. One example is shown in Fig. 5, which demonstrates the formation of FePt in amorphous SiO_2 . The x-ray diffraction results show lines consistent with the fct phase of FePt, and the nanoparticles formed are randomly oriented. Particle sizes up to 30 nm in diameter are seen in Fig. 5b, and the largest particles are located in a band near the ions projected range. The particle size and microstructure are strongly dependent on the Pt concentration in the alloy. Magnetic properties of $\text{Fe}_{1-x}\text{Pt}_x$ nanoparticles in SiO_2 are shown in Fig. 6. In Fig. 6a, the magnetization measurements for the $\text{Fe}_{61}\text{Pt}_{39}$ alloy are clearly not saturated even at a field of 65 kOe, so that the magnetic coercivity derived from this measurement (>25 kOe) is a lower limit only. Prominent shoulders at $H = 0$ are observed in the hysteresis loop, and their origin requires further

investigation. The variation of H_c with Pt concentration is shown in Fig. 6b. The coercivity reaches a maximum of ~ 28 kOe in the range of 40%–45% Pt in the alloy. Detailed results for the SiO_2/FePt system will be reported separately.

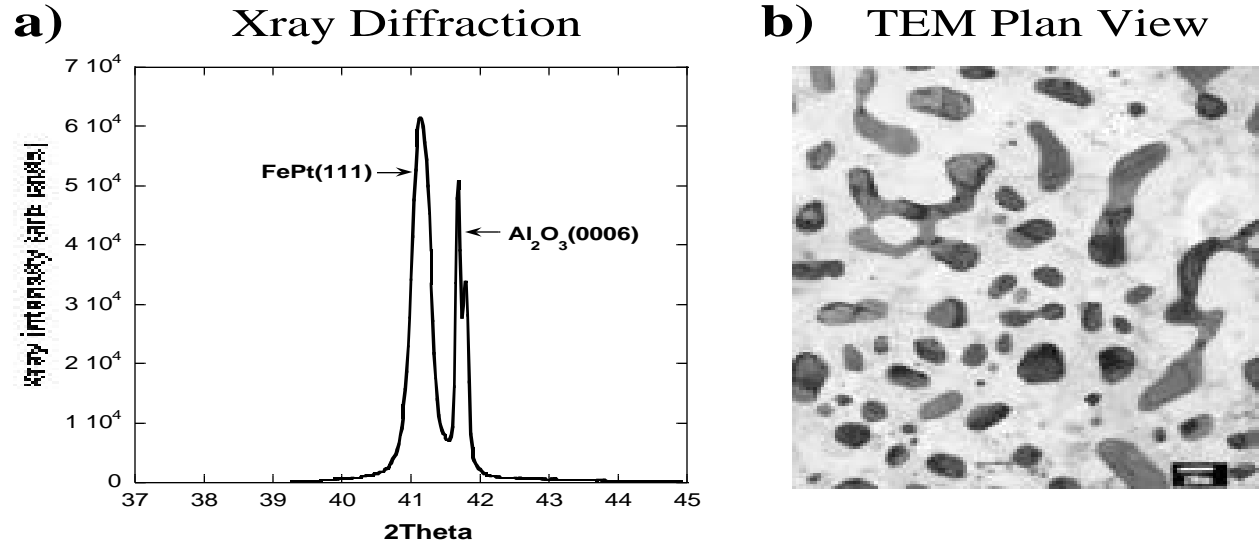


Figure 4. X-ray diffraction (a) and plan view TEM (b) for $\text{Fe}_{55}\text{Pt}_{45}$ nanoparticles formed in Al_2O_3 by implantation at 200°C followed by annealing ($1100^\circ\text{C}/2$ h/Ar + 4% H_2). In (b), the scale bar is 200 nm.

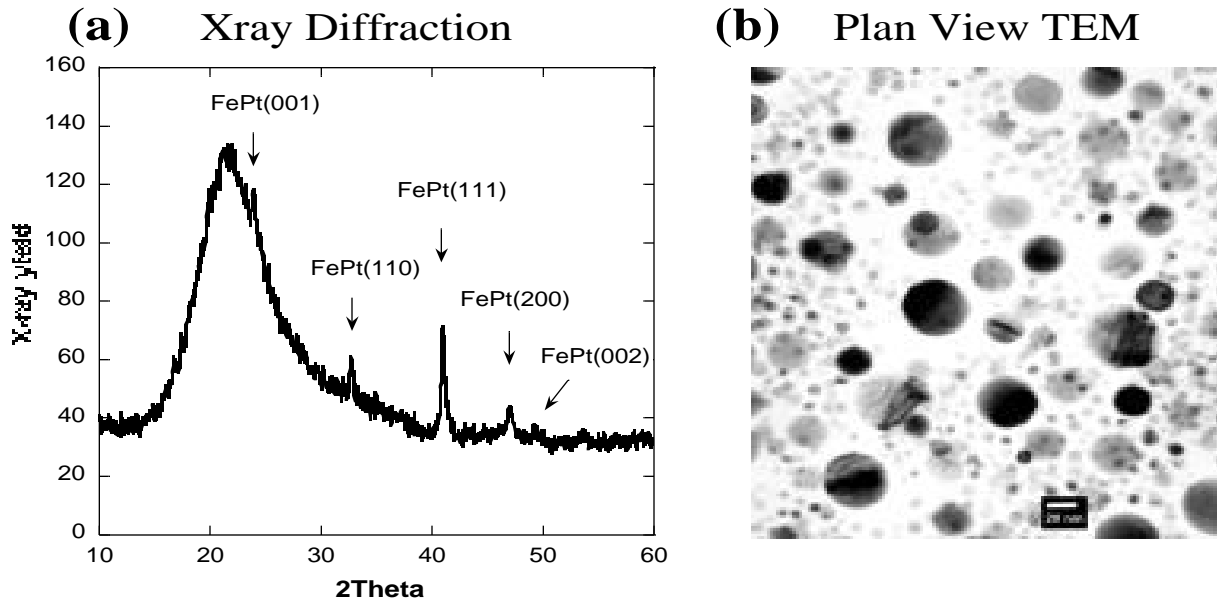


Figure 5. X-ray diffraction (a) and plan view TEM (b) for $\text{Fe}_{55}\text{Pt}_{45}$ nanoparticles formed in amorphous SiO_2 by room-temperature implantation followed by annealing ($1000^\circ\text{C}/2$ h/Ar + 4% H_2). In (b), the scale bar is 20 nm.

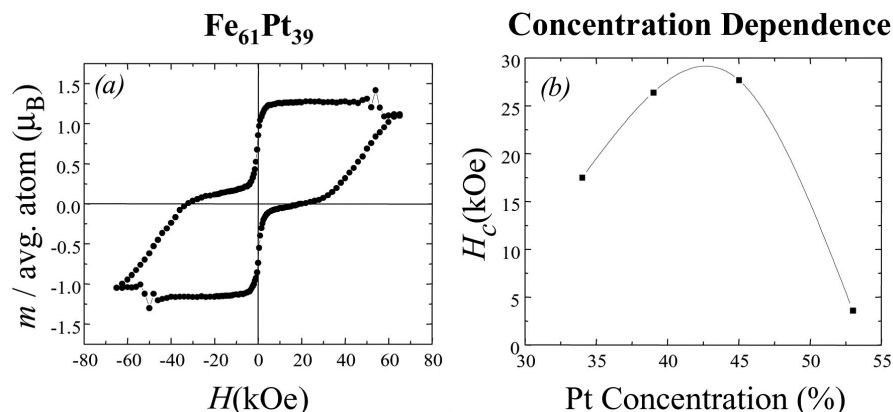


Figure 6. Magnetic properties (at 5 K with H parallel to the surface normal) for Fe_{1-x}Pt_x nanoparticles in SiO₂. A magnetization curve for Fe₆₁Pt₃₉ is shown in (a). The dependence of H_c on Pt concentration in the alloy is shown in (b).

In summary, ferromagnetic Fe_{1-x}Pt_x nanoparticles with extremely high coercivities have been produced in Al₂O₃ by ion implantation and annealing. Implantation at high temperatures (500°C) followed by thermal annealing gives rise to small FePt nanoparticles (max size 25 nm) that exhibit multiple orientations, whereas implantation at 200°C for the same dose gives rise to large particles with a single orientation (<111> FePt parallel to the Al₂O₃ c-axis). In both cases, the magnetic coercivities are extremely high (>20 kOe) at 5 K, and they remain in excess of 18 kOe at room temperature. Ferromagnetic FePt nanoparticles have also been formed in SiO₂. Magnetic coercivities approaching 30 kOe have been achieved in SiO₂, but the hysteresis loops have pronounced shoulders at H = 0. Further work is necessary to clarify this behavior.

ACKNOWLEDGMENTS

Oak Ridge National Laboratory, managed by UT-Battelle, LLC, for the U.S. Dept. of Energy under contract DE-AC05-00OR22725.

REFERENCES

1. D. Weller, A. Moser, L. Folks, M. E. Best, W. Lee, M. F. Toney, M. Schwickert, J.-U. Thiele, and M. F. Doerner, *IEEE Trans. on Magnetics* **36**, 10 (2000).
2. S. Sun, C. B. Murray, D. Weller, L. Folks, and A. Moser, *Science* **287**, 1989 (2000). See also *IEEE Trans. on Magnetics* **37**, 1239 (2001).
3. M. Watanabe, T. Masumoto, D. H. Pink, and K. Hono, *Appl. Phys. Lett.* **76**, 3971 (2000).
4. B. Bain, D. Laughlin, K. Sato, and Y. Hirotsu, *J. Appl. Phys.* **87**, 6962 (2000).
5. C. P. Luo and D. J. Sellmyer, *Appl. Phys. Lett.* **75**, 3162 (1999).
6. C. P. Luo, S. H. Liou, L. Gao, Y. Liu, and D. J. Sellmyer, *Appl. Phys. Lett.* **77**, 2225 (2000).
7. C.-M. Kuo and P. C. Kuo, *J. Appl. Phys.* **87**, 419 (2000).
8. C. W. White, S. P. Withrow, J. D. Budai, L. A. Boatner, K. D. Sorge, J. R. Thompson, K. S. Beaty, and A. Meldrum, *Nucl. Inst. and Methods B* (in press).
9. I. Panagiotopoulos, S. Stavroyiannis, D. Niachos, J. A. Christodoulides, and G. C. Hadjipanayis, *J. Appl. Phys.* **87**, 4358 (2000).
10. T. Goto, Y. Ide, H. Abe, K. Watanabe, J. Onagawa, H. Yoshida, and J. M. Cadogan, *J. Mag. and Mag. Materials* **198-199**, 486 (1999).